Int. J. Solids Structures, 1974, Vol. 10, pp. 1017–1034. Pergamon Press. Printed in Gt. Britain.

FINITE EXTENSIONAL DEFORMATION OF A RIGID PLASTIC ARCH

DONALD A. DADEPPO

Department of Civil Engineering and Engineering Mechanics,
The University of Arizona, Tucson, Arizona 85721, U.S.A.

and

ROBERT SCHMIDT

Department of Civil Engineering,
University of Detroit, Detroit, Michigan 48221, U.S.A.

(*Received* 16 *August* 1973; *revised* 4 *January* 1974)

Abstract—The exact, nonlinear extensional theory of a rigid perfectly plastic arch is used to determine the complete load-deflection behavior of a clamped semicircular arch under the action of a vertical upward point load at the crown. A rate formulation of the problem is discussed. Solution of the rate problem at the yield-point state provides the basis for the construction of exact solutions for thin and for thick arches. Numerical results are presented in graphical form. These results consist of load-deflection curves for three thin arches and one thick arch. The plots together with formulas presented herein show that the slope of the load-deflection curve at the yield-point state is nonzero and positive for upward loading. This result deviates from the zero slope predicted by the usual methods of limit analysis in which geometry changes are neglected.

NOTATION

a	radius of centroidal circle of undeformed arch
$\dot{e}$	rate of extensional strain of the centroidal line
H	one half the depth of arch cross section
K	$(\sqrt{2}+1)+(\sqrt{2}-1)/\alpha$
l	length of plastically deformed region of zero curvature
M	internal bending moment on a cross section of the arch
M_0	yield moment of cross section of the arch
m	M/M_0
N	internal normal force on a cross section of the arch
N_0	normal yield force of the cross section of the arch
n	N/N_0
P	vertical point load applied at crown
P_y, P_{fp}, P_{ult}	values of P: at yield point state, when arch first becomes fully plastic, and the ultimate load, respectively
P_L	$4(\sqrt{2}+1)M_0/a$, the yield load for an inextensional arch
s_0, s	arc length measured along the underformed and deformed centroidal lines respectively
t	time
u	component of displacement at load point in the direction of P
$\dot{v}, \dot{w}$	tangential and normal components of velocity
x, y	rectangular coordinates of a point on the deformed centroidal line
α	H/a, depth ratio
β	$\dfrac{\partial\Phi}{\partial M}\Big/\dfrac{\partial\Phi}{\partial N}$
γ	angular position of a plastic hinge at the yield-point state
θ	subtending angle of an undeformed segment of arch

$\bar{\kappa}$ curvature of centroidal line
μ non-negative multiplier appearing in mathematical statement of flow rule
ϕ angle of inclination of tangent to centroidal line
Φ yield function
ψ rotation of a plastic hinge.

Superposed dot indicates partial derivative of a function with respect to time with s_0 held constant. Square brackets denote the difference in the values of a function just ahead and just behind a point of discontinuity in the function, $[f] = f^+ - f^-$.
The Δ symbol denotes the difference between corresponding quantities in two solutions of the rate equations.
$\Delta f = f_2 - f_1$ where f_2 and f_1 are solution functions.

INTRODUCTION

When geometry changes are taken into account it is found that in general the post-yield quasi-static deformation of a plastic structure must take place under increasing or decreasing load rather than under constant load as predicted by the methods of limit analysis in which geometry changes are neglected. Thus, the analysis of post-yield deformations is of interest to the engineer concerned with the reserve strength of structures such as arches which may undergo significantly large deformations.

The main features of a general approach to the analysis of the quasi-static finite deformation of a plastic solid have been described by Onat[1]. The method consists in formulating the analysis as a boundary-value problem in terms of rates of deformation and rates of stress with respect to the current configuration and state of stress. Knowing the rates (i.e. rates of stress and deformation and the corresponding velocity field) at time t one can determine the mechanical state of the solid a short time later. By repeated formulation and solution of the rate problem one can determine numerically the load-deformation history in a step-by-step fashion. Criteria for uniqueness of the solution of the rate problem and for the stability of equilibrium, and an application of the theory to the analysis of the yield-point state of a rigid-plastic inextensional arch have been given by Onat[1]. The step-by-step method of solution is not always necessary. Onat and Shu[2] were able to construct the complete load-deformation history of a rigid-plastic inextensional arch with large deflections on the basis of information obtained by solving the rate problem at the yield-point state. Because the effect of axial force on the plastic behavior of the arch was neglected their analysis predicts an unrealistic, asymptotic load-deflection relation at large values of the load.

A formulation of the rate problem for the analysis of the quasi-static extensional finite deformation of an arch made of an elasto-plastic material has been given by DaDeppo[3]. The particular equations and the results of an analysis for the case of an arch composed of a rigid–plastic material are presented herein.

PROBLEM

The problem to be considered is the determination of the post-yield, quasi-static load-deformation behavior of a uniform clamped semicircular arch under the action of a monotonically increasing vertical concentrated force $P(t)$ applied at the crown as shown in Fig. 1 for a thin arch at the yield-point state. The arch is assumed to have a symmetric sandwich type cross-section of depth $2H$ (Fig. 2a). It is assumed that the facings develop all of the resistance to the bending couple M and the axial force N, while the core provides the required resistance to the shear force Q. The positive senses for the stress resultants M, N and Q are as shown in Fig. 3. For the ideal sandwich section composed of a rigid perfectly

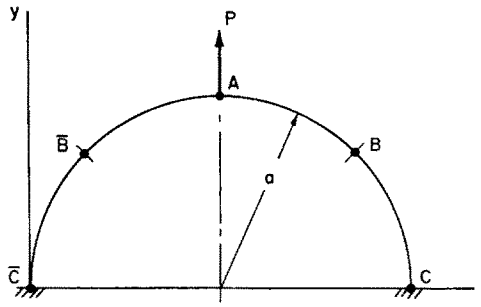

Fig. 1. Arch at yield-point state.

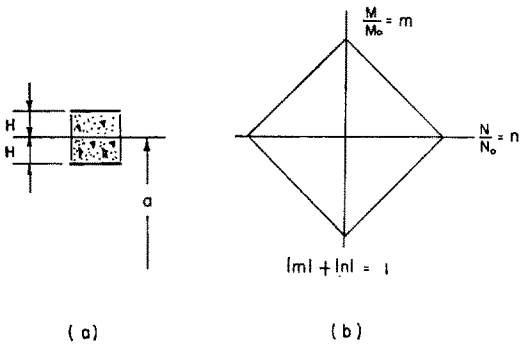

Fig. 2. Cross section and yield condition.

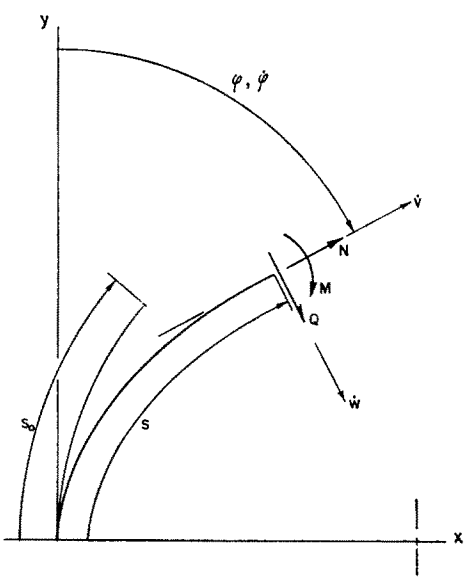

Fig. 3. Geometry and forces.

plastic material the bending moment-axial force interaction curves for initial yield and for the fully plastic states coincide (Fig. 2b). In this paper the rate of plastic strain is determined by the plastic potential flow rule. With the bending moment and axial force as generalized stresses, the corresponding generalized rates of strain are the rate of curvature and the rate of extensional strain of the centroidal line which are denoted as $\dot{\kappa} = \partial\dot{\phi}/\partial s$ and $\dot{e}$, respectively. Herein, the rate of extensional strain is understood to be the time rate of change of natural (logarithmic) strain.

The independent variables employed in describing the mechanical state of the arch are arc length s_0 (a material coordinate) measured along the undeformed centroidal line and time, t. Arc length s in the deformed state is

$$s = s(s_0, t). \tag{1}$$

The mechanical state of the arch may also be described in terms of current arc length s and time t. In this case equation (1) together with the identity $t = t$ may be regarded as representing a coordinate transformation. To achieve compactness in the equations a superposed dot is used to designate the partial derivative with respect to time of a function of s_0 and t. Thus if $f = f(s_0, t)$, then

$$\dot{f} \equiv \frac{\mathrm{d}f}{\mathrm{d}t} = \left(\frac{\partial f}{\partial t}\right)_{s_0}.$$

We note that if equation (1) is employed to express f in terms of s and t, then

$$\dot{f} = \frac{\partial f}{\partial s}\dot{s} + \frac{\partial f}{\partial t}.$$

The natural strain is

$$e = \ln\left(\frac{\mathrm{d}s}{\mathrm{d}s_0}\right) = -\ln\left(\frac{\partial s_0}{\partial s}\right) \tag{2}$$

from which, by differentiation, one obtains

$$\dot{e} = \frac{\partial \dot{s}}{\partial s_0}\Big/\frac{\partial s}{\partial s_0} = \frac{\partial \dot{s}}{\partial s} \tag{3}$$

and

$$\frac{\mathrm{d}}{\mathrm{d}t}\left(\frac{\partial s_0}{\partial s}\right) = -e\frac{\partial s_0}{\partial s}. \tag{4}$$

The angle of inclination of the tangent to the reference line in the deformed state with respect to the y-axis (Fig. 3) is $\phi(s_0, t)$. Thus, the curvature is

$$\bar{\kappa} = \frac{\partial \phi}{\partial s} = \frac{\partial \phi}{\partial s_0}\frac{\partial s_0}{\partial s} \tag{5}$$

from which we obtain

$$\dot{\bar{\kappa}} = \frac{\partial \dot{\phi}}{\partial s} + \frac{\partial \phi}{\partial s_0}\left(\frac{\partial \dot{s}_0}{\partial s}\right). \tag{6}$$

By using the notation $\dot{\kappa} = \dfrac{\partial \dot{\phi}}{\partial s}$ and equation (4), one can rewrite this result in the form

$$\dot{\bar{\kappa}} = \dot{\kappa} - \dot{e}\bar{\kappa}. \tag{7}$$

Let the yield condition be expressed in the general form

$$\Phi(M, N) = C > 0 \tag{8}$$

so that

$$\dot{\Phi} = \frac{\partial \Phi}{\partial M}\dot{M} + \frac{\partial \Phi}{\partial N}\dot{N}. \tag{9}$$

Then, by the plastic potential flow law we may summarize the mechanical behavior of the arch at any section as follows:

$$\begin{aligned} &\dot{e} = \dot{\kappa} = 0 \quad \text{when} \quad \Phi < C, \quad \text{and when} \quad \Phi = C \quad \text{and} \quad \dot{\Phi} < 0, \\ &\dot{e} = \mu \frac{\partial \Phi}{\partial N}, \qquad \dot{\kappa} = \mu \frac{\partial \Phi}{\partial M} \quad \text{when} \quad \Phi = C \quad \text{and} \quad \dot{\Phi} = 0 \end{aligned} \tag{10}$$

where μ is a non-negative number. Equations (10) must be modified if the yield condition has corners and the stress point (M, N) lies in a corner. The necessary modifications are described in[4]. At an isolated plastic hinge the rate of curvature and rate of strain are undefined. At such sections $\dot{e}$ and $\dot{\kappa}$ in equations (10) are to be replaced by $[\dot{v}]$ and $[\dot{\phi}]$, respectively, where the bracket notation is used to indicate the difference in the values of the bracketed quantity just ahead and just behind a hinge and $\dot{v}$ is the component of the velocity tangential to the deformed centroidal line (Fig. 3). Thus, $[\dot{v}] = \dot{v}^+ - \dot{v}^-$, $[\dot{\phi}] = \dot{\phi}^+ - \dot{\phi}^-$, and

$$\begin{aligned} &[\dot{v}] = [\dot{\phi}] = 0 \quad \text{when} \quad \Phi < C, \quad \text{and when} \quad \Phi = C \quad \text{and} \quad \dot{\Phi} < 0 \\ &[\dot{v}] = \mu \frac{\partial \Phi}{\partial N}, \qquad [\dot{\phi}] = \mu \frac{\partial \Phi}{\partial M} \quad \text{when} \quad \Phi = C \quad \text{and} \quad \dot{\Phi} = 0. \end{aligned} \tag{10a}$$

The deformed shape of the arch can be determined by geometrical means if $\phi(s_0, t)$ and $s(s_0, t)$ are specified, since

$$\frac{\partial x}{\partial s} = \sin \phi, \quad \frac{\partial y}{\partial s} = \cos \phi. \tag{11}$$

Therefore, in view of equations (2) and (5) the problem of determining the quasi-static deformations of the arch amounts to the determination of the field variables $\phi(s_0, t)$, $s(s_0, t)$, $M(s_0, t)$, $N(s_0, t)$, and $Q(s_0, t)$ such that the constitutive equations (10) and/or (10a), the equations of equilibrium,

$$\begin{aligned} &\frac{\partial N}{\partial s} - Q\frac{\partial \phi}{\partial s} = 0 \\ &\frac{\partial Q}{\partial s} + N\frac{\partial \phi}{\partial s} = 0 \\ &\frac{\partial M}{\partial s} + Q = 0 \end{aligned} \tag{12}$$

and the boundary conditions are satisfied. Since the displacements at the supports must vanish, two conditions are obtained by integration of equations (11).Thus,

$$2a = \int_0^{s_1} \sin \phi \, ds, \qquad 0 = \int_0^{s_1} \cos \phi \, ds \tag{13}$$

where s_1 is the total length of the deformed reference line. Also, there can be no rotation at the supports of the clamped arch, hence

$$\phi_{C^-} = 0, \qquad \phi_{C^+} = \pi \tag{14}$$

where $\phi_{C^-}(\phi_{C^+})$ is the inclination (with respect to the y-axis) of the tangent to the centroidal line at the section just behind (in front) of the left (right) support. Equilibrium at the load point requires that

$$\begin{aligned} P + [N\cos\phi - Q\sin\phi] &= 0 \\ [N\sin\phi + Q\cos\phi] &= 0. \end{aligned} \tag{15}$$

In deriving these equations the possibility of ϕ being discontinuous at the load point was considered. If ϕ is continuous at the load point and if the deformation is symmetric then for the semicircular arch $\phi = \pi/2$ at the load point and in this case (15) reduces to

$$P - [Q] = 0, \qquad [N] = 0. \tag{16}$$

The second of equations (16) states that the axial force is continuous at the load point.

RATE PROBLEM

An analysis which takes into account geometry changes shows that in general the post-yield quasi-static deformation of a rigid perfectly plastic structure must proceed under increasing or decreasing load rather than under constant load as predicted by the methods of limit analysis in which geometry changes are neglected. Clearly, the relationship of rate of loading to rate of deformation is of interest, especially at the yield-point state. The relationship can be obtained by solving a boundary value problem which involves rates of stress, rates of deformation and rate of loading. Onat[1] has explained how the solution of the rate problem can be applied to the analysis of finite deformation by means of a step-by-step numerical method. Onat[1] has also pointed out that by solving the rate problem at the yield-point state one may determine which one of possibly several competing kinematically admissible velocity fields is the incipient velocity field which characterizes the mode of deformation from the yield-point state.

Equations governing rates for quasi-static deformation are obtained by partial differentiation of the equations of equilibrium (12) with respect to time with s_0 held constant. Thus, in view of equation (2)

$$\begin{aligned} &\frac{\partial \dot{N}}{\partial s} - Q\frac{\partial \dot{\phi}}{\partial s} - \dot{Q}\frac{\partial \phi}{\partial s} = 0 \\ &\frac{\partial \dot{Q}}{\partial s} + N\frac{\partial \dot{\phi}}{\partial s} + \dot{N}\frac{\partial \phi}{\partial s} = 0 \\ &\frac{\partial \dot{M}}{\partial s} + \dot{Q} + \dot{e}Q = 0. \end{aligned} \tag{17}$$

At a section where a yield hinge forms, $\dot{\phi}$ and $\dot{v}$ may be discontinuous and the rates just in front and just behind the hinge must satisfy the relations

$$\begin{aligned} [\dot{N}] - [Q\dot{\phi}] &= 0 \\ [\dot{Q}] + [N\dot{\phi}] &= 0 \\ [\dot{M}] + [Q\dot{v}] &= 0. \end{aligned} \tag{18}$$

Equations (18) were derived under the assumption that ϕ is continuous at least until hinge action begins. At the load point the second of equations (18) must be replaced by

$$[\dot{Q}] + [N\dot{\phi}] - \dot{P} = 0. \tag{19}$$

Equations (18) and (19) are obtained by considering, at t and at $t + \mathrm{d}t$, the equilibrium of an element of material that contains the section at which the yield hinge forms.

The rate of strain $\dot{e}$ and rate of rotation $\dot{\phi}$, expressed in terms of normal and tangential components of velocity and the curvature (Fig. 3) are

$$\begin{aligned} \dot{e} &= \frac{\partial \dot{v}}{\partial s} - \bar{\kappa}\dot{w} \\ \dot{\phi} &= \frac{\partial \dot{w}}{\partial s} + \kappa \dot{v}. \end{aligned} \tag{20}$$

Equations (20) may be derived by considering the change in geometry, in time $\mathrm{d}t$, of an element of material whose deformed length at time t is $\mathrm{d}s$ and noting that the extension of the element in time interval is $\dot{e}\mathrm{d}t$. At the boundaries, because of the clamped supports,

$$\dot{\phi}_{C^-} = \dot{v}_{C^-} = \dot{w}_C = 0, \qquad \dot{\phi}_{C^+} = \dot{v}_{C^+} = \dot{w}_C = 0. \tag{21}$$

Finally, the rates of deformation must satisfy the constitutive equations (10).

In general the rate problem may have more than one solution, hence, the question of uniqueness is of interest. A sufficient condition for uniqueness is established by following Hill[5] and Onat[1]. First, we observe that each solution of the rate problem and the difference between any two solutions must satisfy equations (17), (18), (20) and (21). In addition, where $\Phi = C$ the solutions and their differences must satisfy the conditions

$$\dot{e} = \beta\dot{\kappa} \tag{22}$$

at a section where $\dot{\phi}$ is continuous, and at an isolated hinge

$$[\dot{v}] = \beta[\dot{\phi}] \tag{22a}$$

where

$$\beta = \frac{\partial\Phi}{\partial M}\Big/\frac{\partial\Phi}{\partial N}, \quad \text{and} \quad \dot{e} = \dot{\kappa} = [\dot{v}] = [\dot{\phi}] = 0$$

at all sections where $\Phi < C$. For the piecewise linear yield condition shown in Fig. 2(b), $\beta = \pm H$. Now, multiply the first, second and third of equations (17) by $\dot{v}$, $\dot{w}$ and $\dot{\phi}$, respectively, add, and integrate over the current length of the arch. Integrating by parts and taking into account the equations of equilibrium (12) and (16), and equations (18–22) yields, after some involved manipulations,

$$\int \{\dot{N}\dot{e} + \dot{M}\dot{\kappa}\}\,\mathrm{d}s + \int \{N\dot{\phi}^2 - 2Q\dot{e}\dot{\phi}\}\,\mathrm{d}s + \Sigma\{\dot{M}[\dot{\phi}] + \dot{N}[\dot{v}]\} - \Sigma\beta[Q\dot{\phi}^2] - \beta_P P\dot{\phi}_P^2 = \dot{P}\dot{u} \tag{23}$$

where the integrals extend over the current length of the arch and the summations extend over all plastic hinges. In equation (23), $\dot{P}$ is the prescribed rate of loading, $\dot{\phi}_P$ is the rate of rotation of the section at which P is applied, $\dot{u}$ is the component of velocity in the direction of $\dot{P}$, $\dot{M}$ and $\dot{N}$ are the stress rates at a plastically deforming hinge where $\dot{\phi}$ is discontinuous, and the brackets have the meaning given previously. We note here that ϕ was

assumed to be continuous in deriving equation (23). Let $\Delta\dot{M}$, $\Delta\dot{N}$, $\Delta\dot{\phi}$, etc. designate the differences in corresponding quantities in two solutions of the rate problem. Then, by repeating the calculations which led to equation (23), one obtains

$$\int \{\Delta\dot{N}\,\Delta\dot{e} + \Delta\dot{M}\,\Delta\dot{\kappa}\}\,ds + \int \{N(\Delta\dot{\phi})^2 - 2Q\,\Delta\dot{e}\,\Delta\dot{\phi}\}\,ds + \Sigma\{\Delta\dot{M}[\Delta\dot{\phi}] + \Delta\dot{N}[\Delta\dot{v}]\} - \Sigma\beta[Q(\Delta\dot{\phi})^2] - \beta_P P(\Delta\dot{\phi}_P)^2 = \Delta\dot{P}\,\Delta\dot{u}. \quad (24)$$

Since the rate of loading $\dot{P}$ is prescribed, $\Delta\dot{P} = 0$ and the right hand side of equation (24) is zero. It can be shown by using equations (10) and (10a) that $\Delta\dot{N}\,\Delta\dot{e} + \Delta\dot{M}\,\Delta\dot{\kappa} \geq 0$, $\Delta\dot{N}[\Delta\dot{v}] + \Delta\dot{M}[\Delta\dot{\phi}] \geq 0$. Therefore, if there are two distinct solutions of the rate problem their difference must be such that

$$\int \{N(\Delta\dot{\phi})^2 - 2Q\,\Delta\dot{e}\,\Delta\dot{\phi}\}\,ds - \Sigma\beta[Q(\Delta\dot{\phi})^2] - \beta_P P(\Delta\dot{\phi}_P)^2 \leq 0. \quad (25)$$

Suppose now that in a particular situation we can show that

$$\int \{(\Delta\dot{\phi})^2 - 2Q\,\Delta\dot{e}\,\Delta\dot{\phi}\}\,ds - \Sigma\beta[Q(\Delta\dot{\phi})^2] - \beta_P P(\Delta\dot{\phi}_P)^2 > 0 \quad (26)$$

for the differences associated with all distinct admissible velocity fields. Then, there is a contradiction to inequality (25) and the assumption of more than one velocity field which satisfies the rate equation is false. Therefore, inequality (26) is a sufficient condition for uniqueness. It is worthy of note that inequality (26) does not involve stress rates.

FINITE DEFORMATION

The starting point of the analysis is the determination of the yield-point state. Then, the solution of the corresponding rate problem determines the initial tangent to the load deflection relation $P = f(u)$, where u is the component of displacement in the direction of P at the load point. In general the step-by-step numerical procedure would be required to construct the load-deformation relation. For the relatively simple problem considered herein the solution of the rate problem at the yield-point state suggests a trial shape for the equilibrium configuration at finite deformation. The true configuration is obtained by adjustment of the parameters which define the trial configuration. Solution of the rate problem at the yield-point state shows that thin arches and thick arches must be considered separately. An arch is thin if the thickness ratio $\alpha = H/a$ is in the range $0 \leq \alpha < 3 - 2\sqrt{2}$. For thick arches, $3 - 2\sqrt{2} \leq \alpha \leq 1$.

Thin arch, $0 \leq \alpha < 3 - 2\sqrt{2}$

The methods of limit analysis show that the yield load P_y is given by

$$P_y = \frac{4N_0}{K}$$

where

$$K = (\sqrt{2} + 1) + \frac{(\sqrt{2} - 1)}{\alpha}.$$

Since $M_0 = HN_0$ the yield load can also be expressed in the form

$$P_y = \frac{4M_0}{\alpha K a} = \frac{(\sqrt{2} - 1)P_L}{\alpha K}. \quad (27)$$

where $P_L = 4(\sqrt{2}+1)M_0/a$ is the yield load for an inextensional arch. If $\alpha = 0$, αK in equation (27) must be replaced by $\sqrt{2}-1$. As indicated in Fig. 1, the yield condition is satisfied at the load point, the quarter points, and the supports. The stress profile for the yield-point state is shown in Fig. 4. Because of symmetry only points on the right half of the

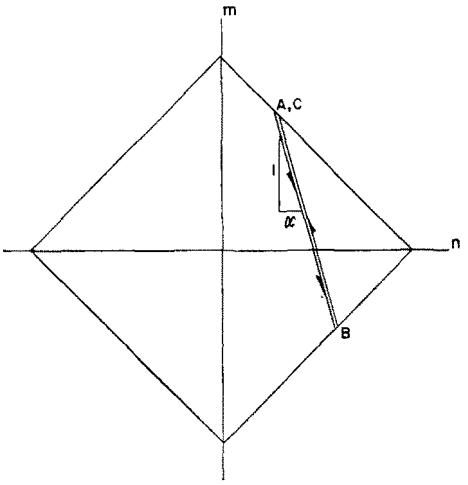

Fig. 4. Stress profile for thin arch at yield-point state.

arch are identified on the stress profile. Equation (27) also defines the yield load for downward loading. For a downward load the signs of all stress resultants are reversed.

The nondimensionalized bending moment and axial forces at A^+ and C^- are

$$m = 1 - \frac{2}{K}, \qquad n = \frac{2}{K},$$

and at B

$$m = -1 + \frac{2\sqrt{2}}{K}, \qquad n = \frac{2\sqrt{2}}{K}.$$

No serious difficulties arise in solving the rate problem at the yield-point state; however, some awkward and lengthy algebraic expressions do come up. For compactness we present only the relation between the rate of load and the rate of displacement for symmetric deformation with hinge action at A^-, A^+, B, $\bar{B}$, C^- and $\bar{C}^+$,

$$\dot{P} = \frac{4\sqrt{2}[\sqrt{2}-1+(\sqrt{2}+1)\alpha^2]}{\alpha^3 K^3(1-\alpha)}\frac{M_0\dot{u}}{a^2}.$$

By employing the definition of P_L, we obtain, for the slope of the load-deflection curve at the yield-point, the relation

$$\frac{dP}{du} = \frac{\dot{P}}{\dot{u}} = \frac{\sqrt{2}[3-2\sqrt{2}+\alpha^2]}{\alpha^3 K^3(1-\alpha)}\frac{P_L}{a} > 0. \tag{28}$$

For an inextensional arch $\alpha = 0$ and equation (28) reduces to the result given by Onat[1]. Equation (28) shows that for the upward loading shown in Fig. 1 motion from the yield-point state must take place under increasing load. For a downward point load, with u positive down, dP/du at the yield-point is the negative of that given by equation (28). Thus, for the downward load the equilibrium at the yield-point state is unstable.

An analysis paralleling that of Onat and Shu[2], in which second order derivatives are examined, can be employed to determine the deformed configuration of the arch in the neighborhood of the yield-point state with greater accuracy than results from solution of the rate problem alone. We do not present an analysis here; we merely note that the analysis shows that:

(1) The hinge at B (and $\bar{B}$) splits into two hinges which travel with respect to the undeformed reference axis. The material between the two hinges is plastically bent and stretched. The curvature of the deformed reference line between two moving hinges is zero and the tangent to the deformed reference line is continuous at a traveling hinge.

(2) The hinges at the load point and at the supports remain stationary. The material adjacent to these hinges is plastically stretched and bent to a curvature $\bar{\kappa} = 1/H$.

The configuration near the yield-point state suggests a symmetric configuration at finite deformation as shown in Fig. 5 for the right half of the arch. Segments of the arch between

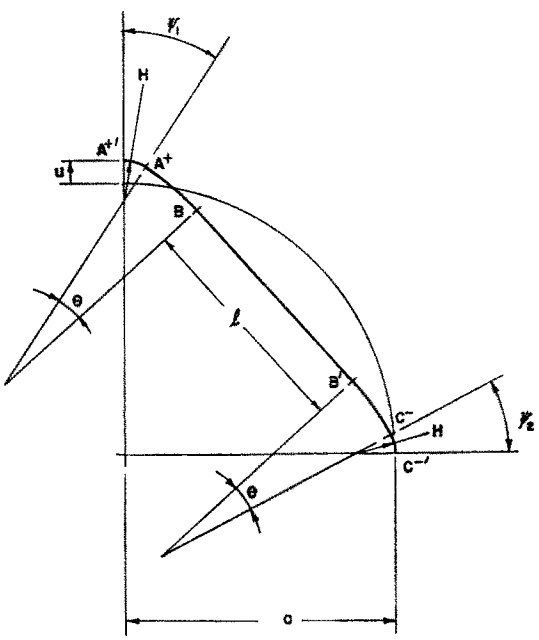

Fig. 5. Thin arch at finite deformation.

$A^{+\prime}$ and A^{+}, between B and B', and between C^{-} and $C^{-\prime}$ have been plastically deformed while the segments between A^{+} and B and between B' and C^{-} are undeformed. The yield condition is satisfied at all points in the plastically deformed regions. The stress profile for the right half of the arch is shown in Fig. 6. Figure 5, with $l = a(1 + \alpha)(\psi_1 + \psi_2)$ shows the

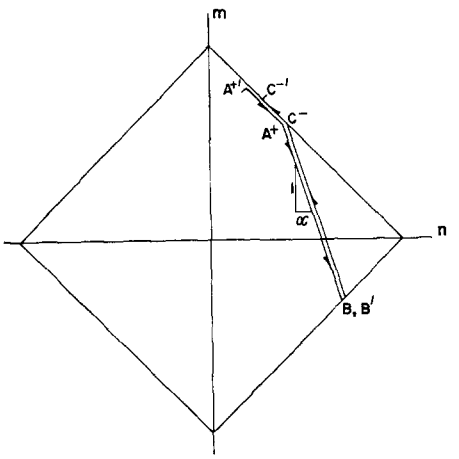

Fig. 6. Stress profile for thin arch at finite deformation.

true configuration which was obtained by adjusting parameters in a more general trial configuration. From the geometry shown in Fig. 5 and the expression for l we obtain the geometric relations:

$$l = a(1+\alpha)\left(\frac{\pi}{2} - 2\theta\right), \tag{29}$$

$$\left(2\sin\theta + \frac{l}{a(1-\alpha)}\right)\cos(\theta + \psi_1) = 1, \tag{30}$$

$$\psi_1 + \psi_2 + 2\theta = \frac{\pi}{2}, \tag{31}$$

$$u = [2a(1-\alpha)\sin\theta + l]\sin(\theta + \psi_1) - a(1-\alpha). \tag{32}$$

From the equations of equilibrium and the yield condition we obtain

$$N_B = \frac{2\alpha}{(1+\alpha) - (1-\alpha)\cos\theta} N_0, \tag{33}$$

$$N_B - M_B = N_0 M_0, \tag{34}$$

$$P = \frac{P_L N_B}{N_0} \frac{(\sqrt{2}-1)}{2\alpha} \sin(\psi_1 + \theta), \tag{35}$$

where N_B and M_B are the moment and thrust in region B, B'.

Equations (29–35) are valid for $0 \leq \theta \leq \pi/4$, and they define the post-yield load-deformation response up to the state for which $\theta = 0$. It can be easily verified, as indicated by the stress profile in Fig. 6, that nowhere is the yield condition violated. The velocity field and stress rates defined by Fig. 5 in conjunction with equations (29–35) satisfy all of the rate equations and the constitutive equations (10). With the aid of inequality (26) it has been established that the solution is unique. We note here that the plastic deformation takes

place at $A^{+\prime}$, B^{-}, $B^{\prime +}$ and $C^{-\prime}$. Also, it is noted that putting $\theta = \frac{\pi}{4}$ in equations (29–35) produces the known result for the yield-point state.

Points on the load-deflection curve are calculated as follows: choose θ and then use equations (29–33) and (35) to calculate l, ψ_1, ψ_2, u, N_B and P, respectively.

The arch becomes fully plastic, i.e. the yield condition is satisfied everywhere as θ decreases to zero; however, the capacity of the arch to sustain still greater loads is not exhausted. The geometry of the arch for $\theta = 0$ and the associated stress profile are shown in Figs. 7 and 8, respectively.

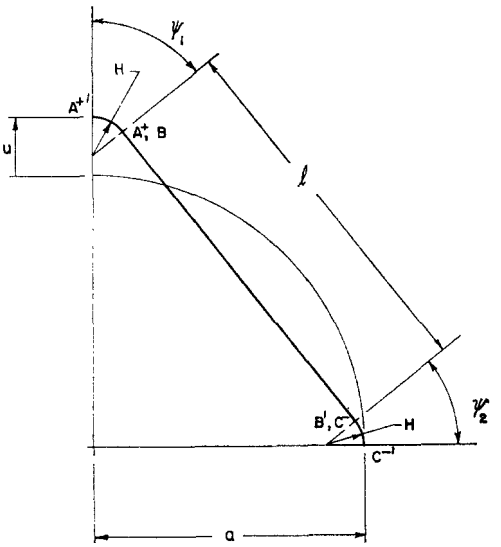

Fig. 7. Configuration of fully plastic thin arch.

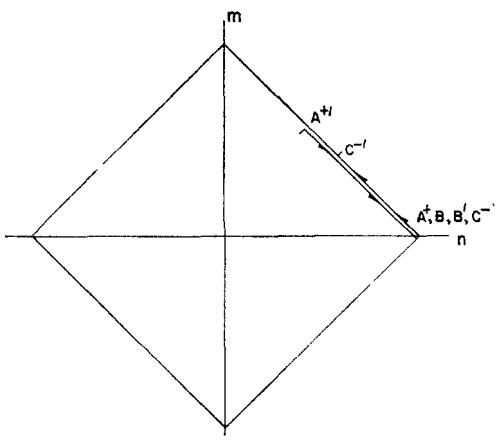

Fig. 8. Stress profile for fully plastic thin arch.

A solution for continuing finite deformation is obtained by assuming that the configuration of the arch in the final stages of deformation is symmetric and as shown in Fig. 7. From geometry, we obtain:

$$\psi_2 = \frac{\pi}{2} - \psi_1, \tag{36}$$

$$l = \frac{a(1-\alpha)}{\cos\psi_1}, \tag{37}$$

$$u = a(1-\alpha)[\tan\psi_1 - 1]. \tag{38}$$

With the assumption that the axial force in the straight portion of the arch remains at N_0, we obtain from the yield condition and equilibrium

$$N_B = N_0, \qquad M_B = 0 \tag{39}$$

$$P = P_L \frac{(\sqrt{2}-1)\sin\psi_1}{2\alpha}. \tag{40}$$

The yield condition is satisfied everywhere and the stress profile remains as shown in Fig. 8.

A velocity field and rates of stress which are compatible with the geometry of Fig. 7 and which satisfy all of the equations of the associated rate problem are obtained by assuming that the hinge action occurs at sections A^+, B and B' with all other sections remaining rigid. At B, the hinge action is a simple extension while at B' there is extension with hinge rotation. The calculations show that the stress points A^+, B, B' and C^- lie in the corner of the yield condition, i.e. not on a side at the corner. The rate problem does not have a unique solution since more than one distribution of admissible plastic rates which satisfy all of the rate equations can be constructed. It is believed that the solution can be shown to be unique in a restricted sense if the distribution of the extensional plastic rates over segment B, B' (Fig. 7) is disregarded in comparing competing velocity fields, i.e. if over B, B' we consider two extensional plastic rate fields to be distinct only if

$$\int \dot{e}_1 \, ds + [\dot{v}_1]_B + [\dot{v}_1]_{B'} \neq \int \dot{e}_2 \, ds + [\dot{v}_2]_B + [\dot{v}_2]_{B'}.$$

Thick arch, $1 > \alpha \geq 3 - 2\sqrt{2}$

At the yield-point state of a thick arch the yield condition is satisfied at the load point and at symmetrically situated points which are located between the load point and the quarter points as shown in Fig. 9. The stress profile for a thick arch at the yield-point state is shown in Fig. 10. The methods of limit analysis show that the location of the hinge at B is given by

$$\sin\gamma = \frac{2\sqrt{\alpha}}{1+\alpha}, \tag{41}$$

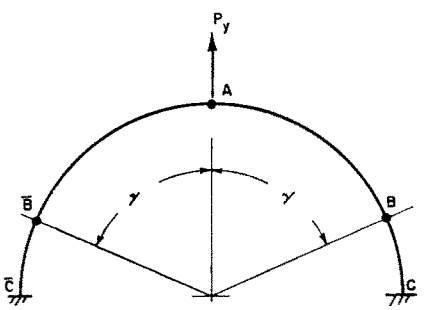

Fig. 9. Thick arch at yield-point state.

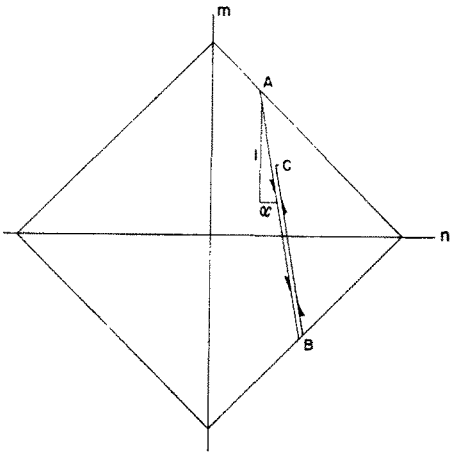

Fig. 10. Stress profile for thick arch at yield-point state.

and the yield load is

$$P_y = 2N_0\sqrt{\alpha}.$$

Using the relations

$$H = \alpha a, \qquad M_0 = HN_0, \quad \text{and} \quad P_L = 4(\sqrt{2}+1)\frac{M_0}{a},$$

we can express P_y in the form

$$P_y = \frac{\sqrt{2}-1}{2\sqrt{\alpha}} P_L. \tag{42}$$

From the solution of the rate problem at the yield-point state, the initial slope of the load-deflection curve is found to be

$$\frac{dP}{du} = \frac{\dot{P}}{\dot{u}} = \frac{(\sqrt{2}-1)(1-\alpha)}{8\alpha^{3/2}}\frac{P_L}{a} > 0. \tag{43}$$

Equations (27) and (42) and equations (28) and (43), respectively yield identical results when the transition value of $\alpha = 3 - 2\sqrt{2}$ is used to evaluate P_y and dP/du at the yield-point state. Equation (42) gives the yield load for downward loading, and equation (43) with a minus sign in front of the right hand side gives the slope of the load-deflection relation for a downward load with u measured positive down. It is seen that for downward loading the equilibrium at the yield-point is unstable. We observe from equation (43) that dP/du tends to zero only in the limiting (and unimportant) case of a very thick arch for which $\alpha = H/a \to 1$.

There are three stages to the post-yield plastic deformation of a thick arch. The second and third stages are the same as the two stages for a thin arch. In the first stage of deformation the hinges at B and $\bar{B}$ split into two pairs of traveling hinges while the hinge at A remains stationary, and the configuration of the arch is as shown in Fig. 11. Segment

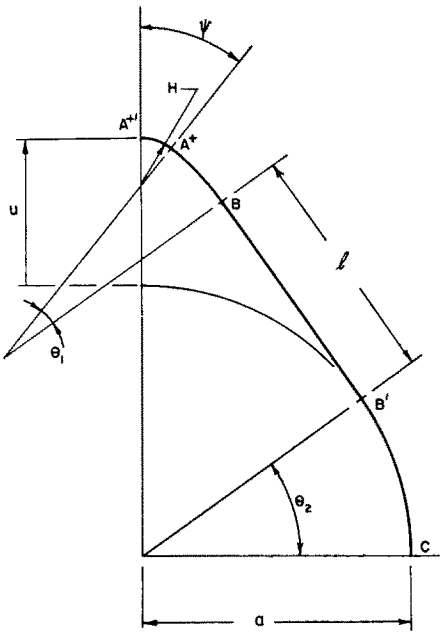

Fig. 11. Thick arch at first stage of finite deformation.

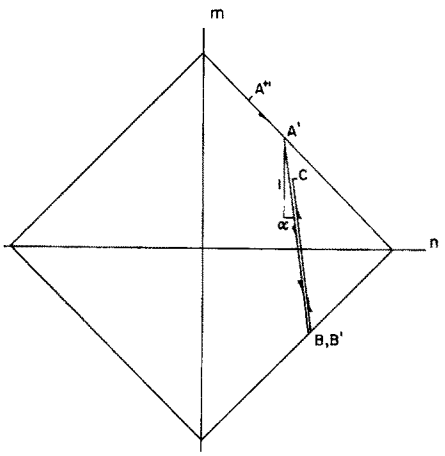

Fig. 12. Stress profile for thick arch during first stage of finite deformation.

$A^{+\prime}$, A^{+} and segment B, B' are plastically deformed while segments A^{+}, B and B', C are rigid. The plastic deformation takes place at $A^{+\prime}$ at B^{-}, and at B'^{+}. With

$$l = a(1+\alpha)\psi, \tag{44}$$

we obtain, from the geometry shown in Fig. 11,

$$\sin\theta_2 = \left(\frac{1-\alpha}{1+\alpha}\right)\left(\frac{\sin\psi}{\psi}\right), \tag{45}$$

$$\theta_1 = \frac{\pi}{2} - \psi - \theta_2, \tag{46}$$

$$u = -a(1-\alpha)(1-\cos\psi) + l\cos\theta_2. \tag{47}$$

From the equations of equilibrium and the yield condition we get

$$N_B = \frac{2\alpha}{(1+\alpha)-(1-\alpha)\cos\theta_1} N_0. \tag{48}$$

$$N_B - M_B = M_0 N_0$$

$$P = \frac{(\sqrt{2}-1)\sin(\psi+\theta_1)}{2\alpha}\frac{P_L N_B}{N_0} \tag{49}$$

in which N_B and M_B are the axial force and bending moment in the straight segment B, B'. The stress profile (Fig. 12) shows that nowhere is the yield condition violated. Equations

(44–49) with $\theta_1 \geq \theta_2$ define the load–deflection response. Initially, $\theta_1 > \theta_2$, and θ_1 decreases until $\theta_1 = \theta_2$, at which time the first stage of plastic deformation is complete.

Equations (29–35) define the response in the second stage of deformation during which $\theta_1 \to 0$ and the arch becomes fully plastic.

Equations (36–40) define the response in the last stage of deformation.

RESULTS AND CONCLUSIONS

Calculations were carried out for thick and thin arches. Load–deflection curves are presented in Fig. 13. The curve $\alpha = 0$ is the load–deflection curve for an inextensional arch; it is identical to that obtained previously by Onat and Shu[2]. This curve is asymptotic to the line

$$u = a\left(\frac{\pi^2}{4} - 1\right)^{1/2} - a.$$

For all arches the load and corresponding deflection at which the arch first becomes fully plastic may be calculated from the relations

$$P_{fp} = \frac{\sqrt{2}-1}{2\alpha}\left[1 - \frac{4}{\pi^2}\left(\frac{1-\alpha}{1+\alpha}\right)^2\right]^{1/2} P_L,$$

$$u_{fp} = a(1+\alpha)\left[\frac{\pi^2}{4} - \left(\frac{1-\alpha}{1+\alpha}\right)^2\right]^{1/2} - a(1-\alpha)$$

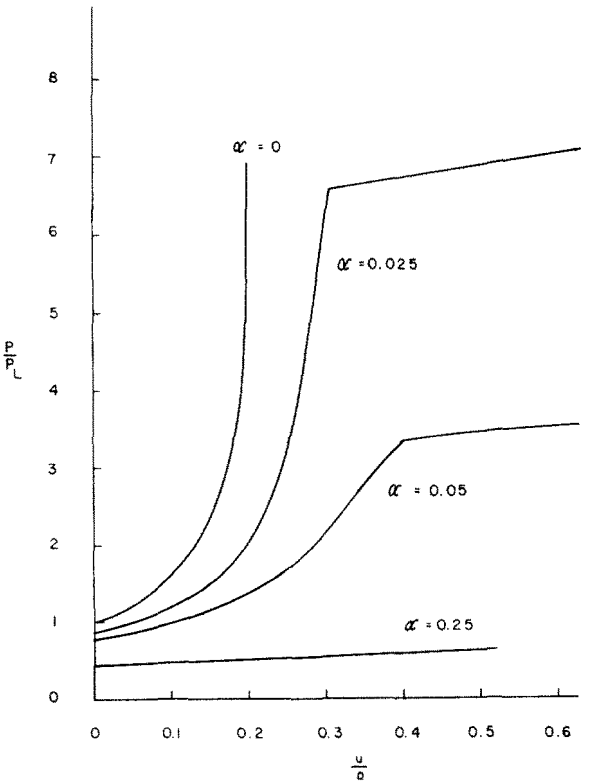

Fig. 13. Load–deflection curves, P/P_L vs u/a.

and the ultimate load is

$$P_{ult} = \frac{\sqrt{2}-1}{2\alpha} P_L.$$

Numerical values for P_{fp}, u_{fp} and P_{ult} are given in Table 1.

Table 1. Loads and deflections

α	P_y/P_L	P_{fp}/P_L	u_{fp}/a	P_{ult}/P_L
0	1	∞	0·211	∞
0·025	0·873	6·59	0·306	8·28
0·050	0·774	3·38	0·398	4·14
0·250	0·414	0·76	1·815	0·83

For the thick arch with $\alpha = 0{\cdot}25$, the load and deflection at which hinge action is initiated at the supports are $P = 0{\cdot}518P_L$ and $u = 0{\cdot}275a$, respectively. To avoid, misinterpretation of the numerical results we recall that

$$P_L = 4(\sqrt{2}+1)\frac{M_0}{a} = 4(\sqrt{2}+1)\alpha N_0$$

increases with increasing thickness ratio for constant N_0. Therefore, for arches with $\alpha \neq 0$, the ultimate load, expressed in terms of N_0 is $P_{ult} = 2N_0$. In Fig. 14 the load–deflection

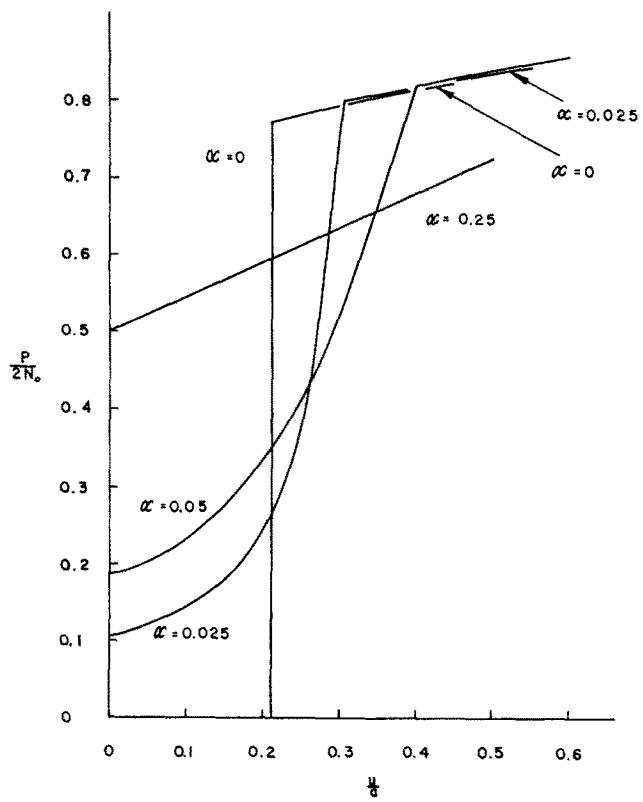

Fig. 14. Load–deflection curves, $P/2N_0$ vs u/a.

curves are plotted with $P/2N_0$ vs u/a. The curves show that for a fixed amount of material (as measured by N_0), the initial yield load and the load at any deflection up to approximately $u = 0{\cdot}25a$ increases with increasing depth of arch.

In this study it has been assumed that the effect of shear on the yield load capacity of a cross section of arch is negligible. However, in Ref.[6] it is shown that the effect of shear on the load carrying capacity of a simply supported beam is negligible for depth-to-span ratio less than about one-fifth, which, for a semicircular arch, corresponds to a value of $\alpha = 0{\cdot}3$. From this we conclude that the results presented herein should be sufficiently accurate for applications to thin and to moderately thick arches, with an upper limit of $\alpha = 0{\cdot}3$. For $\alpha > 0{\cdot}3$ (very thick arch), the combined effects of shear, moment and thrust must be taken into account.

Acknowledgements—This investigation was supported by the National Science Foundation Grant GK-19726 and by the U.S. Naval Civil Engineering Laboratory, Port Hueneme, California.

REFERENCES

1. E. T. Onat, *Plasticity* (edited by E. H. Lee and P. S. Symonds), p. 225. Pergamon Press, New York (1960).
2. E. T. Onat and L. S. Shu, *J. appl. Mech.* **29**, 549 (1962).
3. D. A. DaDeppo, *Rep.* on Contract NBy-32254, Research Institute of Science and Engineering, University of Detroit, Detroit (1965).
4. J. N. Goodier and P. G. Hodge, *Elasticity and Plasticity*. Wiley, New York (1958).
5. R. Hill, *J. Mech. Phys. Solids* **5**, 153 (1957).
6. P. G. Hodge, *Plastic Analysis of Structures*. McGraw-Hill, New York (1959).

Абстракт — Применяется точная, нелинейная теория удлинения для жесткой, идеально пластичной арки, с целью определения полного поведения нагрузки и прогиба жесткой, полукруглой арки, под влиянием вертикальной, направленной вверх нагрузки в ключе. Обсуждается формулировка скорости для этой задачи. Решение задачи скорости для состояния точки текучести является основной для построения точных решений для тонких и толстых арок. Даются численные результаты в графической форме. Эти результаты заключают кривые для зависимости нагрузка-прогиб, для трех тонких арок и одной толстой арки. Графики, вместе с представленными здесь формулами, указывают ненулевый и положительный наклон кривой нагрузка-прогиб, для состояния точки текучести, при нагрузке направленной вверх. Этот результат отклоняется от нулевого наклона, предсказанного обыкновенными методами анализа предельного состояния, в которых пренебрегаются изменениями геометрии.